IOP Publishing Journal of Physics: Condensed Matter

J. Phys.: Condens. Matter **22** (2010) 084026 (8pp) doi:10.1088/0953-8984/22/8/084026

Quasi-one-dimensional metals on semiconductor surfaces with defects

Shuji Hasegawa

Department of Physics, School of Science, University of Tokyo, 7-3-1 Hongo, Bunkyo-ku, Tokyo 113-0033, Japan[1]

E-mail: shuji@surface.phys.s.u-tokyo.ac.jp

Received 23 November 2009
Published 5 February 2010
Online at stacks.iop.org/JPhysCM/22/084026

Abstract

Several examples are known in which massive arrays of metal atomic chains are formed on semiconductor surfaces that show quasi-one-dimensional metallic electronic structures. In this review, Au chains on Si(557) and Si(553) surfaces, and In chains on Si(111) surfaces, are introduced and discussed with regard to the physical properties determined by experimental data from scanning tunneling microscopy (STM), angle-resolved photoemission spectroscopy (ARPES) and electrical conductivity measurements. They show quasi-one-dimensional Fermi surfaces and parabolic band dispersion along the chains. All of them are known from STM and ARPES to exhibit metal–insulator transitions by cooling and charge-density-wave formation due to Peierls instability of the metallic chains. The electrical conductivity, however, reveals the metal–insulator transition only on the less-defective surfaces (Si(553)–Au and Si(111)–In), but not on a more-defective surface (Si(557)–Au). The latter shows an insulating character over the whole temperature range. Compared with the electronic structure (Fermi surfaces and band dispersions), the transport property is more sensitive to the defects. With an increase in defect density, the conductivity only along the metal atomic chains was significantly reduced, showing that atomic-scale point defects decisively interrupt the electrical transport along the atomic chains and hide the intrinsic property of transport in quasi-one-dimensional systems.

1. Introduction

One-dimensional structures, in which electrons are confined to move only along a particular direction, are realized as quantum wires, atomic/molecular chains, nanorods, nanotubes, edge states and highly anisotropic organic/inorganic crystals. Most of them are, however, not strictly one-dimensional, but 'quasi-one-dimensional' because electrons can hop to the adjacent chains/wires and/or their widths are not thin enough. Metallic atom chains aligned on surfaces of semiconductor crystals are an example, providing suitable playgrounds for exploring the physics of atomic-scale quasi-one-dimensional metallic systems.

Why are the one-dimensional systems interesting? In general, one-dimensional systems are more easily treated in theoretical calculations than higher dimensions. It is known that analytical solutions, by taking into account strong electron–electron correlations, are obtained only for one-dimensional systems. The theory of a Tomonaga–Luttinger (TL) liquid is an example [1]. Another interesting point is the peculiar electronic states in one-dimensional systems as shown in figure 1. Three-dimensional systems have a density of states (DOS, left column) varying smoothly with energy, while the DOS in lower dimensions changes rapidly as a function of energy. In particular, one-dimensional systems have van Hove singularities with diverging DOS at band edges, which leads to exotic physical properties. About the band dispersion (center column) and Fermi surface (right column), they are isotropic for two and three dimensions, while one-dimensional systems have very anisotropic characters which results in anisotropic transport properties, for example. The Fermi surfaces in one dimension have features suitable for Fermi surface nesting, which induces various phase transitions due to the resulting Fermi surface instability. Fermi surface nesting means large segments of the Fermi surface can be connected to another large segment of another Fermi surface via the reciprocal lattice vector. When the Fermi surface has segments tending to be straight 'lines', the nesting condition is well fulfilled. This condition corresponds to a divergence in the response function, which, in turn, means instability of the system with any perturbations, leading to a transition to a more stable phase.

[1] http://www-surface.phys.s.u-tokyo.ac.jp

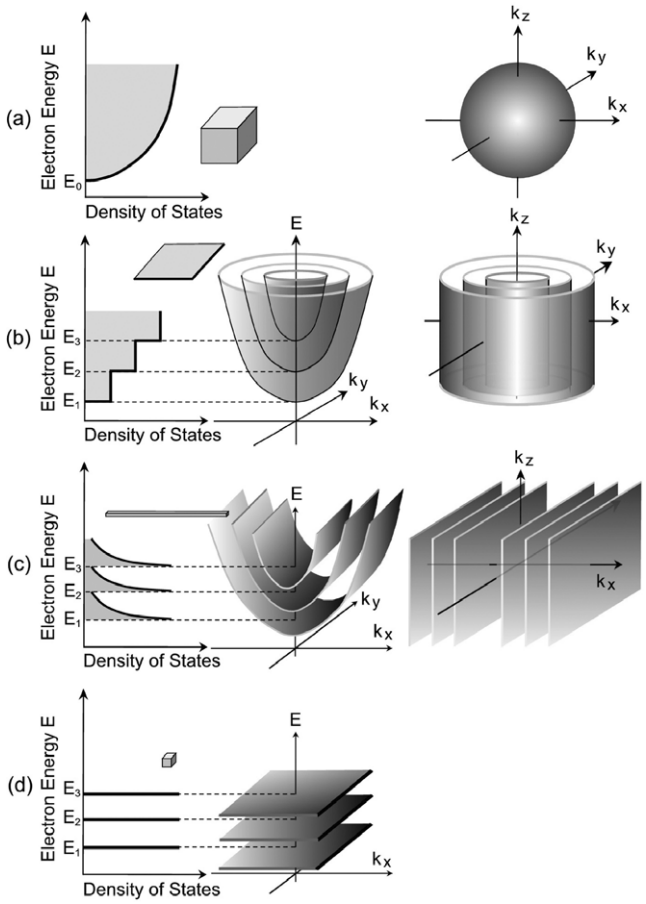

Figure 1. Schematic illustrations of the density of states (left column), band dispersion (center column) and Fermi surfaces (right column) of (a) three-dimensional, (b) two-dimensional, (c) one-dimensional and (d) zero-dimensional free-electron systems.

One-dimensional metallic systems are intrinsically unstable due to large fluctuations and the above-mentioned divergent feature of the Lindhard response function at a wavenumber $2k_F$ (where k_F is the Fermi wavenumber). Due to this electronic instability combined with the electron–lattice interaction, the lattice is periodically distorted and an energy gap opens at the Fermi level. Thus periodic modulations in the electron density and lattice distortion are know as charge-density waves (CDW), resulting in an insulating phase at lower temperature [2]. The insulating character of lower-dimensional systems at low temperature is not only due to the CDW formation, but also by carrier localization due to the strong interference effect.

The most popular phenomenon in one dimension would be the conductance quantization. When carriers flow through a one-dimensional wire in a ballistic way without carrier scattering therein, the conductance is quantized in units of $2e^2/h(= 1/12\,900\ \Omega^{-1})$ [3]. This quantization unit is a universal constant, independent of the material, which is the most striking feature of one-dimensional systems. In the case of ballistic transport in two and three dimensions, the conductance units depend on the Fermi wavenumber k_F which is material-dependent [4].

A theory predicts that, since the scattering angle of a carrier in one dimension is 0° (forward scattering) or 180° (backward scattering) only, the scattering probability is very much reduced, resulting in the enhancement of carrier mobility compared with that in higher dimensions [5]. Accordingly, there are proposals of high-mobility transistors using nanowires. In real one-dimensional systems, however, defects are much more fatal in interrupting the carrier transport than in higher dimensions. This lowers the carrier mobility very much in many one-dimensional systems. Therefore, the present paper discusses the influence of defects in quasi-one-dimensional metallic systems.

In strict one-dimensional systems, electron–electron interaction is essentially important and therefore the one-particle approximation is not applicable. Electrons in one dimension cannot avoid each other nor pass by. The overlap of the electron wavefunction is inevitably maximized at the collision. As a result, the one-particle approximation (Fermi-liquid picture), in which the influence of other electrons is put into the effective potential and one electron is moving therein, fails. Therefore, we need a picture of a TL liquid in which many electrons are always excited collectively. The feature of a TL liquid is confirmed in photoemission spectra and the temperature dependence of electrical conductivity of carbon nanotubes and semiconductor quantum wires [6, 7]. There is no confirmation of a TL liquid, however, for atomic chains on crystal surfaces. Real systems have many other factors such as inter-chain interaction, electron–phonon interaction, CDW formation and various defects, which prevent the systems going into the TL state.

Since magnetic atoms in low-dimensional systems have fewer neighbors, their magnetic moments can become larger than in three dimensions. Also, since the system is intrinsically anisotropic in one dimension, the magnetic anisotropic energy would be larger. In fact, it is shown that magnetic atoms in atomic chains aligned at step edges on a crystal surface have a large magnetic moment [8]. Furthermore, because the screening effect by surrounding carriers is basically weaker in lower dimensions, the Kondo effect and RKKY interaction can extend to longer distances and their features would be enhanced. This would lead to an expectation of 'stronger' diluted magnetic systems in lower-dimensional systems.

Because of many aspects described above, (quasi-)one-dimensional metallic systems are expected to provide much interesting physics. One of the methods for fabricating one-dimensional electronic systems with good controllability is to one-dimensionally confine electrons of a two-dimensional electron gas (2DEG) with an electric field by gate electrodes at the semiconductor interfaces. In the present paper, however, atomic-chain arrays (surface superstructures) formed on semiconductor crystals are introduced to realize quasi-one-dimensional metallic systems. Since the electronic states of such surface superstructures are located within the bandgap of the substrate bulk, the atomic-chain arrays are electronically decoupled from the substrate. Therefore, the carriers in the surface states cannot easily leak into the bulk states of the substrate, and can flow along the surface for a long distance. Of course, the carriers are scattered and leak into the bulk

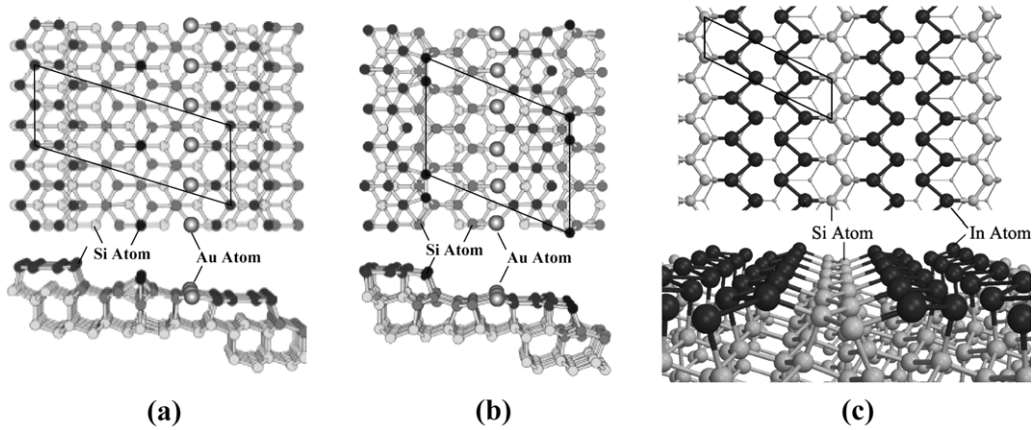

Figure 2. Massive arrays of metal atomic chains on silicon crystal surfaces, formed by depositing one (or less than one) monolayer of metals. (a), (b) Au atomic chains on vicinal Si surfaces (Si(557)–Au, Si(553)–Au) [9]. (c) Indium atomic chains on a flat Si(111) surface (Si(111) 4×1-In surface superstructure) (Si(111)–In) [10].

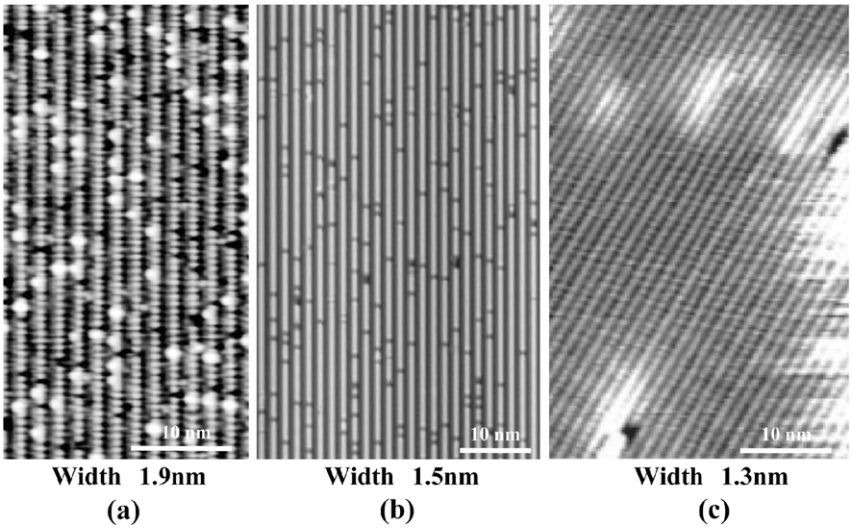

Figure 3. Scanning tunneling microscopy images of the respective chain structures shown in figure 2. (a) Si(557)–Au, (b) Si(553)–Au and (c) Si(111)–In [9, 11, 12].

states if inelastic scattering by defects and phonons occurs, accompanying a large change of energy. So the surface transport property is changed sensitively by surface phase transitions and minute amounts of adatoms and defects, which provide a playground for exploring the rich physics of low-dimensional and nanoscale systems.

First, the atomic and electronic structures of surface systems dealt with in the present paper are introduced in section 2. Then phase transitions clarified so far on the surfaces are described in section 3. Finally, the electrical transport properties measured with surface-sensitive techniques are discussed, by comparing systems with different densities of defects in section 4.

2. Surface quasi-one-dimensional metallic systems

Figure 2 shows examples of surface superstructures with monolayer-metal atoms adsorbed on Si crystals, exhibiting quasi-one-dimensional metallic states. (a) and (b) are 0.2 monolayer Au atoms adsorbed on vicinal surfaces of Si, while (c) is single-monolayer In atoms adsorbed on an Si(111) flat surface. All of them show atomic-chain structures in which metal atoms are aligned along particular crystal orientations. As described below, the systems are metallic only along the atomic chains. Their STM images are shown in figure 3, revealing periodically aligned stripes which consist of the metal atom chains. Their periodicities are 1.9 nm, 1.5 nm and 1.3 nm, respectively. One can notice point defects which are irregularly sitting on the stripes. The defects are observed as bright protrusions on the Si(557)–Au surface, while they are dark depletions on Si(553)–Au. One find few defects on the Si(111)–In surface. These defects are not avoidable even by optimizing the sample preparation conditions, so that the systems look stable thermodynamically by including the defects. As described in section 4, the difference in defect density decisively affects the transport properties.

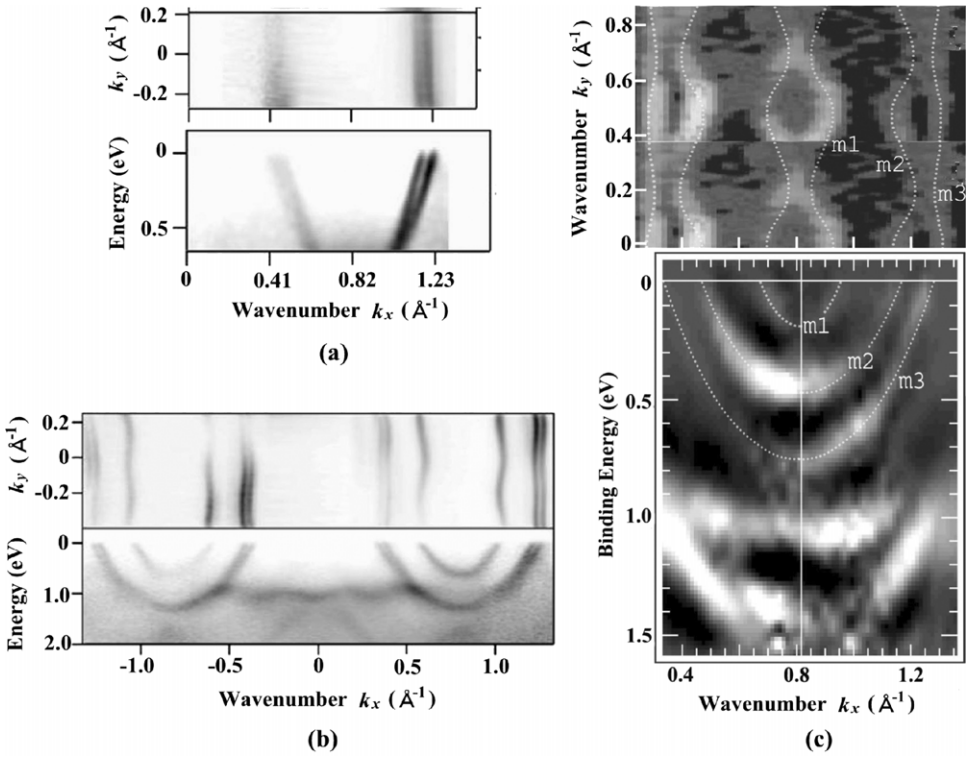

Figure 4. Fermi surfaces (upper panel) and band dispersion diagrams (lower panel) of the respective chain structures shown in figure 2. These are the results of angle-resolved photoemission spectroscopy: (a) Si(557)–Au, (b) Si(553)–Au and (c) Si(111)–In [9, 13–15].

Figure 4 shows the Fermi surfaces (upper panels) and band dispersion diagrams (lower panels) of these three surfaces. These were obtained by ARPES measurements. The Fermi surface of Si(557)–Au is straight lines (Fermi lines), as illustrated in figure 1(c), meaning an ideal one-dimensional metal [9]. Si(553)–Au shows slightly wavy Fermi lines, indicating some inter-chain interaction [13]. Si(111)–In has more wavy Fermi lines, meaning a larger probability of electrons hopping to the adjacent In atomic chains [14, 15]. All of these surfaces have Fermi surfaces having one-dimensional nature, exhibiting the Fermi surface nesting more or less and phase transitions thereby, as shown in the next section.

The band dispersion along the metal atomic chains is parabolic for all surfaces, meaning nearly-free-electron-like states only along the atomic chains. These bands do not show significant dispersion in the direction perpendicular to the chains. These features of electronic states mean that quasi-one-dimensional metallic systems are realized on semiconductor substrates. Every surface has multiple parabolic bands, which originate for different reasons, such as different atomic bondings and spin–orbit interaction. In particular the two proximate bands of the Si(557)–Au surface were first proposed to be spinon–holon bands which are characteristic of a TL liquid [16]. Later, however, it turned out that they are spin-split bands due to spin–orbit interaction [17]. All of them shown here are Fermi-liquid systems.

3. Surface phase transitions

It is shown by Yeom *et al* that these surfaces exhibit phase transitions due to Fermi surface nesting [18–21]. Figure 5(c) shows STM images of Si(557)–Au surfaces at room temperature and low temperature [18]. The atomic chains indicated by arrows show a change that the periodicity in the brightness modulation is doubled at 78 K compared to 300 K. The periodicity doubling corresponds to the Fermi lines in figure 4(a) which bisect the Brillouin zone. Similar double-periodicity modulations along the chains are also observed on Si(111)–In at low temperature, as shown in figure 5(e) [20]. This also corresponds to the m2 and m3 bands in figure 4(c) which approximately bisect the Brillouin zone. Figure 5(d) shows the temperature dependence of the low-energy electron diffraction (LEED) pattern taken from the Si(553)–Au surface [19]. Half-order streaks and one-third streaks (indicated by arrows) appear at low temperatures, which indicate structural modulation of double and triple periodicities along the atomic chains. These correspond to the proximate Fermi lines bisecting the Brillouin zone and the Fermi lines located at 1/3 of the Brillouin zone, respectively, in figure 4(b). In other words, the phase transitions shown here are changes into modulated structures having the super-periodicities corresponding to Fermi surface nesting. Therefore, all of them are believed to be CDW phase transitions.

Figure 5(a) illustrates the band dispersion and atomic arrangement (a: lattice constant) of a one-dimensional free-electron system. The band is occupied by electrons up to the Fermi energy (E_F) and the Fermi wavenumber (k_F). In this example, k_F is exactly half of the zone boundary $k = \pi/a$. The electron density is homogeneous along the atomic chain at higher temperature. Once this chain is cooled down, however, an energy gap opens at E_F and a new zone boundary is formed

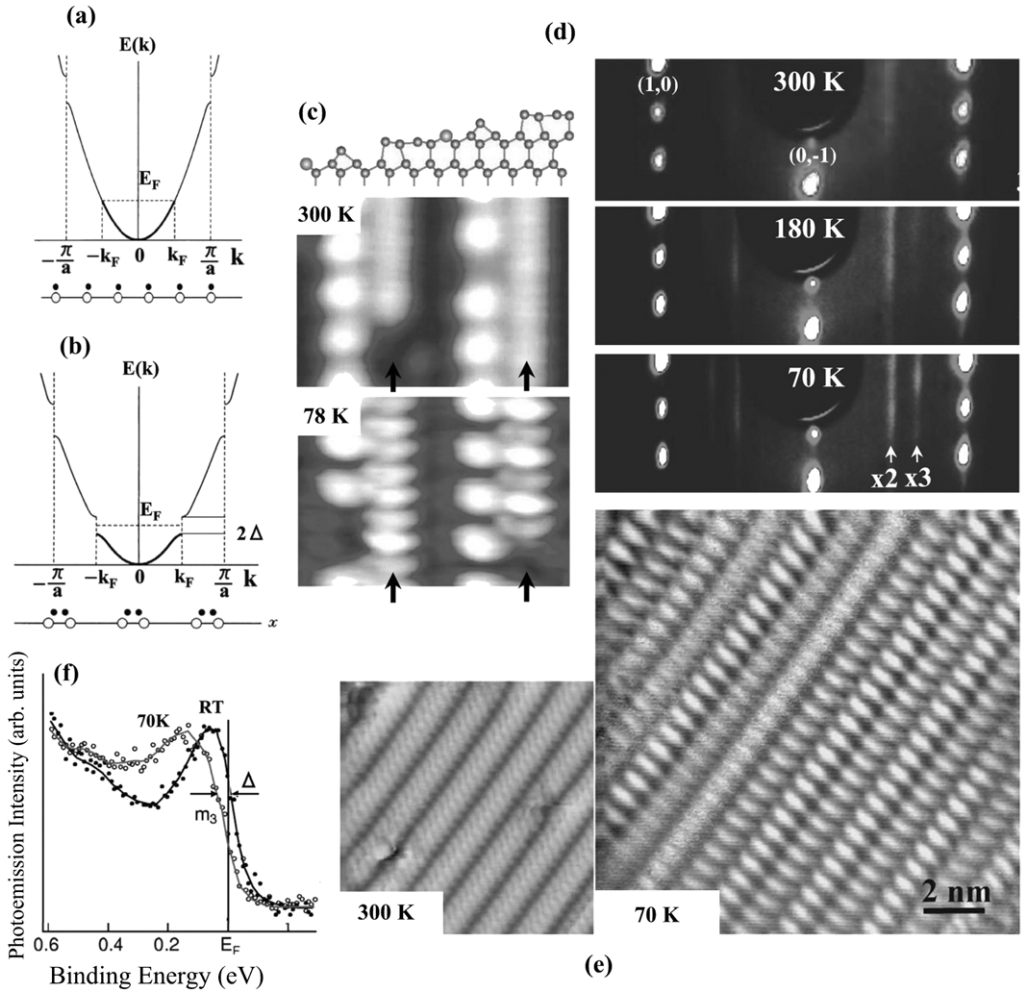

Figure 5. Phase transitions found on the respective chain structures shown in figure 2. (a), (b) Schematics of band dispersion and atomic arrangement of a one-dimensional metal in the metallic phase at higher temperature and in the charge-density-wave phase at lower temperature, respectively. (c) STM images of the Si(557)–Au surface at RT and 78 K [18]. (d) LEED patterns of the Si(553)–Au surface at RT and lower temperatures [19]. (e), (f) STM images [20] and photoemission spectra [21] of the Si(111)–In surface at RT and 70 K.

at $k = k_F$ and the size of the Brillouin zone becomes half, as shown in figure 5(b). This is nothing other than an insulator. The atomic positions slightly shift as shown in figure 5(b) to make the periodicity of the lattice double and to modulate the electron density with the same periodicity. The electron-rich part and the electron-deficit part are alternately arranged with the double periodicity. This is a CDW state, and this phase transition is called the Peierls transition, or CDW transition in general. The brightness modulations observed in the STM images of figures 5(c) and (e) are the spatial distribution of electron density along the atomic chains. Figures 5(a) and (b) illustrate an example of the Fermi surface bisecting the Brillouin zone. When the Fermi surface is located at 1/3 of the Brillouin zone, the lattice distortion and charge-density modulation have the triple periodicity, and the size of the Brillouin zone is reduced to be 1/3.

Figure 5(f) shows photoemission spectra taken from the Si(111)–In surface at room temperature and 70 K [21]. It shows a metallic edge (Fermi edge) at room temperature, while the edge shifts away from E_F at 70 K. This means an energy gap opening at E_F and the system becomes an insulator as shown in figure 5(b). Si(557)–Au as well as Si(553)–Au surfaces shows similar changes in photoemission spectra by cooling. Thus, all of them exhibit metal–insulator transitions due to the Peierls transition which is characteristic of quasi-one-dimensional metals.

4. Surface electronic transport

Figure 6 shows electrical resistance (and conductance) of these surfaces measured as a function of temperature. The resistance was measured with microscopic four-point probes having a probe spacing around 10 μm [23]. Because of the small probe spacing, the measurements are very surface-sensitive. As shown in figures 6(b) and (c), Si(553)–Au and Si(111)–In retain low resistances during cooling from room temperature, while they show drastic increases in resistance below about 130 K [22, 23]. This exactly corresponds to the metal–insulator transitions due to Peierls instability, as described in the previous section. Since the Si bulk crystal shows a completely different temperature dependence of resistance, the

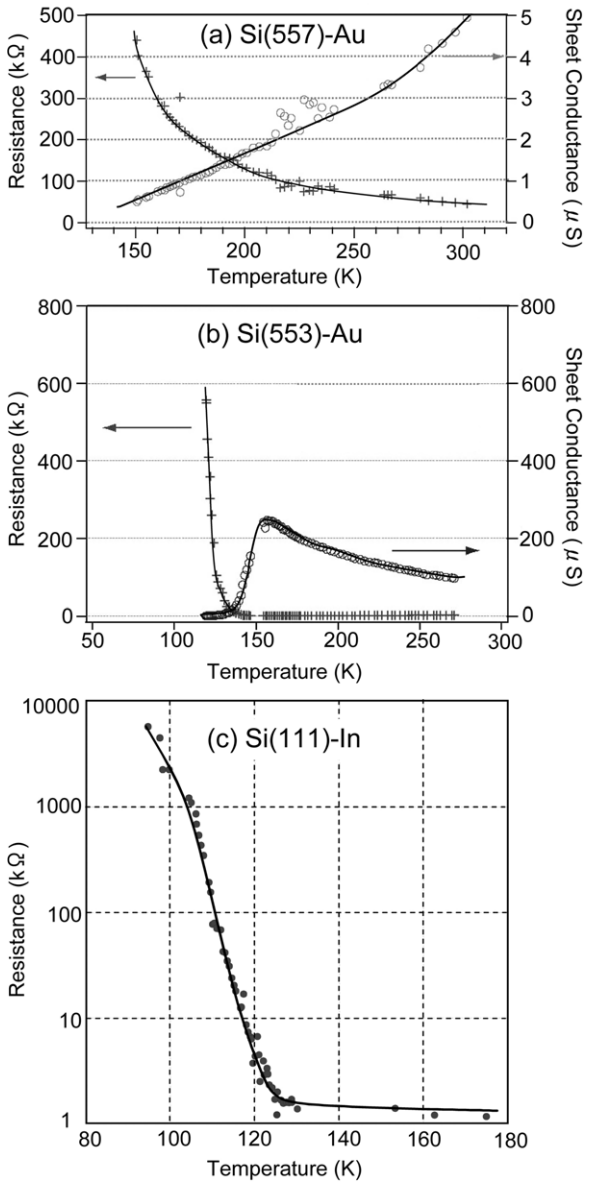

Figure 6. Temperature dependences of the resistance (and sheet conductivity) of the respective chain structures shown in figure 2 [22, 23].

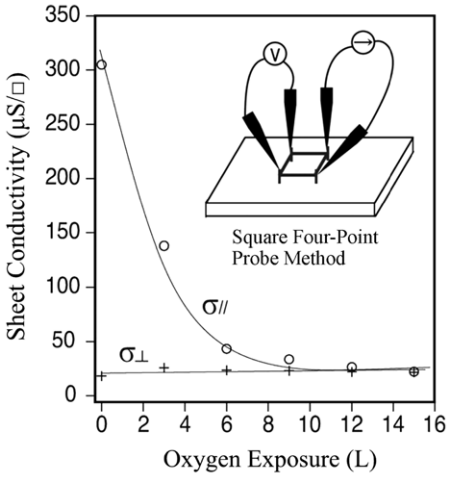

Figure 7. The sheet conductivity along the metallic chains ($\sigma_{\parallel}$) and that in the perpendicular direction ($\sigma_{\perp}$), measured at RT by the square-four-point probe method for the Si(111)–In surface on exposure to oxygen gas [26].

Table 1. The experimental values at RT and calculated values of the sheet conductivity along the metallic chains ($\sigma_{\parallel}$), those in the perpendicular direction ($\sigma_{\perp}$), and their ratios ($\sigma_{\parallel}/\sigma_{\perp}$), for the respective chain structures shown in figure 2. The conductivities were calculated from the Fermi surface and band dispersion (figure 4) by using the Boltzmann equation (equation (1)). Inter-chain interaction estimated by the shape of Fermi surfaces, the average lengths of chain segments divided by the point defects on the chains and the temperature dependence of the electrical conductivity of the respective surfaces are also summarized [25].

	Si(557)–Au		Si(553)–Au		Si(111)–In	
	Exp.	Cal.	Exp.	Cal.	Exp.	Cal.
$\sigma_{\parallel}$ (μS/□)	10	200	82	600	710	240
$\sigma_{\perp}$ (μS/□)	3.5	0.26	30	6.4	13	13
Anisotropy ($\sigma_{\parallel}/\sigma_{\perp}$)	2.9	770	2.7	94	54	19
Inter-chain interaction (shape of Fermi surface)	Weak		Intermediate		Strong	
Segment length (nm)	∼5		∼10		∼100	
Temp.-dep. conductivity	Insulating		*M–I* transition		*M–I* transition	

resistances measured in figures 6(b) and (c) are those of the surface states of the massive array of metal chains.

Interestingly, however, Si(557)–Au shows a quite different temperature dependence, as shown in figure 6(a). The resistance monotonically increases with cooling from room temperature. This result means that the surface is insulating, even at room temperature, and shows no phase transition at all. This, however, contradicts the ARPES results in figure 4 showing a metallic Fermi surface at room temperature and a metal–insulator transition below room temperature. Why does the transport property of Si(557)–Au contradict the electronic structure?

When, in four-point probe resistance measurements, the four probes are arranged in a square on the sample surface, as shown in the inset of figure 7, anisotropy in conductance can be measured [24]. By this 'square four-point probe' method, the sheet conductivity along the metal chains ($\sigma_{\parallel}$) and that in the perpendicular direction ($\sigma_{\perp}$) can be measured separately [24]. The results for the three surfaces are summarized in table 1 [25].

Furthermore, since the Fermi surface and band dispersion near the Fermi level are know as shown in figure 4, the conductivities, $\sigma_{\parallel}$ and $\sigma_{\perp}$, can be calculated by using the following equation which is derived from the Boltzmann equation. The conductivities calculated from the Fermi surface and band dispersion are also included in table 1:

$$\sigma_{ij} = \frac{e^2\tau}{2\pi^2\hbar}\int_{FS}\frac{v_i v_j}{|v|}\mathrm{d}k, \qquad (1)$$

where the group velocity v_i in the i direction ($i = \parallel, \perp$) is derived from the band dispersion $E(\vec{k})$ by $v_i = 1/\hbar \cdot \partial E/\partial k_i$.

The $v_{\parallel}$ and $v_{\perp}$ are the group velocity along the metal chains and that in the perpendicular direction, respectively. The diagonal components of the conductivity tensor σ_{ij} are $\sigma_{\parallel}$ and $\sigma_{\perp}$. The integral of equation (1) is performed on the Fermi surface (FS). τ is the carrier relaxation time, which was assumed to be independent of direction. The values of τ were derived experimentally from the peak width in the photoemission spectra.

Straight Fermi lines in Si(557)–Au as shown in figure 4(a) mean a very small value of $v_{\perp}$, resulting in a small value of $\sigma_{\perp}$, while it has a very large value of $\sigma_{\parallel}$. This high anisotropy is natural for a quasi-one-dimensional system. By comparing the calculated values of $\sigma_{\parallel}$ and $\sigma_{\perp}$ (and its ratio $\sigma_{\parallel}/\sigma_{\perp}$, anisotropy) with the directly measured values, one can find some interesting features. As for the Si(111)–In surface, the calculated and measured values of the ratio $\sigma_{\parallel}/\sigma_{\perp}$ are roughly of the same order, while the measured values of the ratio $\sigma_{\parallel}/\sigma_{\perp}$ from Si(557)–Au and Si(553)–Au surfaces are lower than those of the calculated values by two orders of magnitude. Judging from the degree of straightness of the Fermi lines in figure 4, Si(557)–Au should have the highest value of anisotropy in conductivity (ratio $\sigma_{\parallel}/\sigma_{\perp}$) and Si(111)–In should have the lowest anisotropy in conductivity. The tendency in the measured values is, however, opposite. This is because the measured values of $\sigma_{\parallel}$ in Si(557)–Au and Si(553)–Au are lower than the calculated values by more than one order of magnitude. In particular, the discrepancy between the measured and calculated values is very large for Si(557)–Au. What is the reason for this discrepancy?

One speculation for it is the point defects observed in the STM images of figure 3: the defects are assumed to cut the atomic chains into short segments. Since ARPES clearly reveals metallic bands for all the three surfaces, the segments remain metallic, though the length is shortened. The mean lengths of the segments between two point defects were measured from many STM images of the respective surfaces, which results are summarized in table 1. The Si(557)–Au surface has the highest density of defects, resulting in a short mean length of segments, about 5 nm, while the Si(111)–In surface is much less defective, having segments as long as about 100 nm.

By considering the defect density together with the temperature dependence and anisotropy in conductivity, the point defects are considered to hide the intrinsic transport property. Since the electrical conduction occurs mainly along the metallic chains in quasi-one-dimensional metallic systems, the transport is seriously disturbed just by point defects on the chains. This results in the reduction of the measured $\sigma_{\parallel}$. The carriers need an activation energy to overcome the defects and flow through them or to hop into the adjacent metal chains by avoiding the defects. When this kind of activation limits the transport, the temperature dependence of conductivity has an insulating character even though the segments between the defects are metallic. This scenario can explain the findings that Si(557)–Au has an insulating temperature dependence in transport and the measured value of $\sigma_{\parallel}$ is much lower than the values expected from the Fermi surface. Since, on the other hand, Si(553)–Au and Si(111)–In surfaces have much lower densities of point defects, the intrinsic nature of the atomic chains is revealed in the transport property.

In order to confirm the speculation mentioned above, another experiment was conducted in which the least defective Si(111)–In surface was exposed to oxygen gas to introduce defects in a controlled manner, and the conductivities of $\sigma_{\parallel}$ and $\sigma_{\perp}$ were measured *in situ* with the square four-point probe method as a function of the oxygen dose. The result is shown in figure 7 [26]. STM images (not shown here) showed an increase in the density of point defects with oxygen dosing. The $\sigma_{\parallel}$ drastically decreased with oxygen dosing, while $\sigma_{\perp}$ remained almost constant. Eventually, the conductivities in both directions became equal to each other, meaning an isotropic surface. This result clearly shows that the point defects interrupt the electrical conduction along the metal atomic chains only. In other words, the transport on the pristine Si(111)–In surface is really one dimensional.

5. Summary

Based on the experimental results of three examples of quasi-one-dimensional metallic surfaces, Si(557)–Au, Si(553)–Au and Si(111)–In, we have discussed the metal–insulator transitions due to Peierls instability, together with the temperature dependence and anisotropy in surface electrical conductivity. As described in textbooks on solid state physics, the Fermi surface nesting corresponded to the periodicity of charge-density waves and the electronic state changed into insulating by the phase transition. The metal–insulator transitions were observed in transport with less-defective surfaces, Si(553)–Au and Si(111)–In only, while Si(557)–Au having a higher density of defects did not exhibit a metal–insulator transition, but an insulating nature over the whole temperature range. We have also compared the directly measured surface conductivities with those expected from the Fermi surfaces and band dispersions. With the increase in defect density, the conductivity only along the metal atomic chains was significantly reduced. In this way, it is shown experimentally that atomic-scale point defects decisively interrupt the electrical transport along the atomic chains and hide the intrinsic property of transport.

Acknowledgments

The series of studies summarized here were supported by The Grant-in-Aid and A3 Foresight Program from The Japan Society of Promotion of Science. It is gratefully acknowledged that the results presented here were obtained by the past and present members in my research group.

References

[1] Kawabata A 2007 *Rep. Prog. Phys.* **70** 219
[2] Gruner G 1994 *Density Waves in Solids* (New York: Addison-Wesley)
[3] Landauer R 1957 *IBM J. Rev. Dev.* **1** 223
[4] Matsuda I *et al* 2004 *Phys. Rev. Lett.* **93** 236801
[5] Sakaki H 1980 *Japan. J. Appl. Phys.* **19** L735
[6] Ishii H *et al* 2003 *Nature* **426** 540

[7] Bockrath M *et al* 1999 *Nature* **397** 598
[8] Gambardella P *et al* 2002 *Nature* **416** 301
[9] Crain J N *et al* 2004 *Phys. Rev.* B **69** 125401
[10] Cho J-H, Oh D-H, Kim K S and Kleinman L 2001 *Phys. Rev.* B **64** 235302
[11] Crain J N *et al* 2006 *Phys. Rev. Lett.* **96** 156801
[12] Park S J *et al* 2005 *Phys. Rev. Lett.* **95** 126102
[13] Crain J N *et al* 2003 *Phys. Rev. Lett.* **90** 176805
[14] Ahn J R, Byun J H, Koh H, Rotenberg E, Kevan S D and Yeom H W 2004 *Phys. Rev. Lett.* **93** 106401
[15] Morikawa H, Matsuda I and Hasegawa S 2004 *Hyomen Kagaku* **25** 407
[16] Segovia P, Rurdie D, Hengsgerger M and Baer Y 1999 *Nature* **402** 504
[17] Losio R *et al* 2001 *Phys. Rev. Lett.* **86** 4632
[18] Ahn J R, Yeom H W, Yoon H S and Lyo I-W 2003 *Phys. Rev. Lett.* **91** 196403
[19] Ahn J R, Kang P G, Ryang K D and Yeom H W 2005 *Phys. Rev. Lett.* **95** 196402
[20] Yeom H W *et al* 1999 *Phys. Rev. Lett.* **82** 4898
[21] Yeom H-W *et al* 2002 *Phys. Rev.* B **65** 241307(R)
[22] Okino H, Matsuda I, Yamazaki S, Hobara R and Hasegawa S 2007 *Phys. Rev.* B **76** 035424
[23] Tanikawa T, Matsuda I, Kanagawa T and Hasegawa S 2004 *Phys. Rev. Lett.* **93** 016801
Tanikawa T, Matsuda I, Hobara R and Hasegawa S 2003 *e-J. Surf. Sci. Nanotechnol.* **1** 50
[24] Kanagawa T *et al* 2003 *Phys. Rev. Lett.* **91** 036805
[25] Okino H 2007 *Doctor Thesis* University of Tokyo (March)
[26] Okino H *et al* 2007 *Phys. Rev.* B **76** 195418